

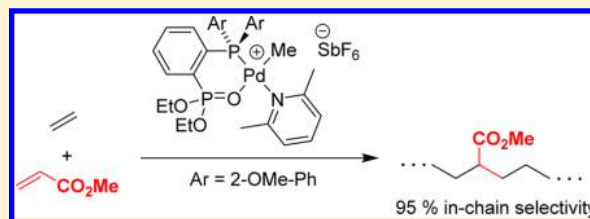
Copolymerization of Ethylene and Methyl Acrylate by Cationic Palladium Catalysts That Contain Phosphine-Diethyl Phosphonate Ancillary Ligands

Nathan D. Contrella, Jessica R. Sampson, and Richard F. Jordan*

Department of Chemistry, The University of Chicago, 5735 South Ellis Avenue, Chicago, Illinois 60637, United States

Supporting Information

ABSTRACT: A series of benzo-linked phosphine-diethyl phosphonate (P-PO) and phosphine-bis(diethyl phosphonate) (P-(PO)₂) ligands and the corresponding (P-PO)PdMe(2,6-lutidine)⁺ and (P-(PO)₂)PdMe(2,6-lutidine)⁺ complexes were synthesized. Cationic (P-PO)PdMe(2,6-lutidine)⁺ complexes are active for ethylene oligomerization/polymerization, with activities of 2 kg mol⁻¹ h⁻¹ for {κ²-1-*P*Pr₂-2-*P*(O)(OEt)₂-5-Me-Ph}PdMe(2,6-lutidine)⁺ (3c), 125 kg mol⁻¹ h⁻¹ for {κ²-1-*P*Ph₂-2-*P*(O)(OEt)₂-5-Me-Ph}PdMe(2,6-lutidine)⁺ (3a), and 1470 kg mol⁻¹ h⁻¹ for {κ²-1-*P*(2-OMe-Ph)₂-2-*P*(O)(OEt)₂-Ph}PdMe(2,6-lutidine)⁺ (3b). The polyethylene is highly linear, with over 80% terminal unsaturation and low (230–1890 Da) molecular weight in all cases. 3b copolymerizes ethylene with methyl acrylate, exhibiting highly selective (95%) in-chain (rather than chain-end) acrylate incorporation. The P-(PO)₂ catalyst {κ²-1-*P*(4-*t*-Bu-Ph)(2-*P*(O)(OEt)₂-5-Me-Ph)-2-*P*(O)(OEt)₂-5-Me-Ph}PdMe(2,6-lutidine)⁺ (3d) is more active for ethylene homopolymerization (2640 kg mol⁻¹ h⁻¹), yielding linear, low-molecular-weight polymer (1280–1430 Da) with predominantly internal olefin placement. In ethylene/methyl acrylate copolymerization, 3d incorporates 2.6 mol % methyl acrylate, 60% of which is in-chain. Both 3b and 3d catalyze ethylene/acrylic acid copolymerization, albeit with low (<10 kg mol⁻¹ h⁻¹) activities and acrylic acid incorporation up to 1.1 mol %.



INTRODUCTION

Palladium(II) alkyl complexes that contain *ortho*-phosphino-arenesulfonate (PO) ligands (A, Chart 1) polymerize ethylene to highly linear polyethylene (PE),¹ and the catalyst activity and the polyethylene molecular weight are strongly influenced by the substituents on the phosphine unit (R) and the lability of the L ligand.² These catalysts also copolymerize ethylene with a wide variety of polar vinyl monomers, yielding functionalized linear copolymers with both in-chain and chain-end incorporation of the comonomer.^{3–8} However, the ethylene polymerization activities and polymer molecular weights exhibited by (PO)PdMeL catalysts are low compared to those for other families of single-site catalysts,⁹ and polar monomers invariably decrease activities and molecular weights.

The combination of a strong (phosphine) and weak (sulfonate) donor in the ancillary PO ligand in (PO)PdR catalysts is believed to suppress β-hydride elimination processes that can lead to chain walking and branched polymer chains^{1,10} and β-X eliminations (X = halide, OR, O₂CR) that can lead to catalyst deactivation in copolymerizations.^{5b,11} Additionally, it has been proposed that the sulfonate group facilitates *cis/trans* isomerization of the catalyst during chain growth via formation of five-coordinate κ³-*P,O,O*-PO species that undergo Berry pseudorotations.^{1,10}

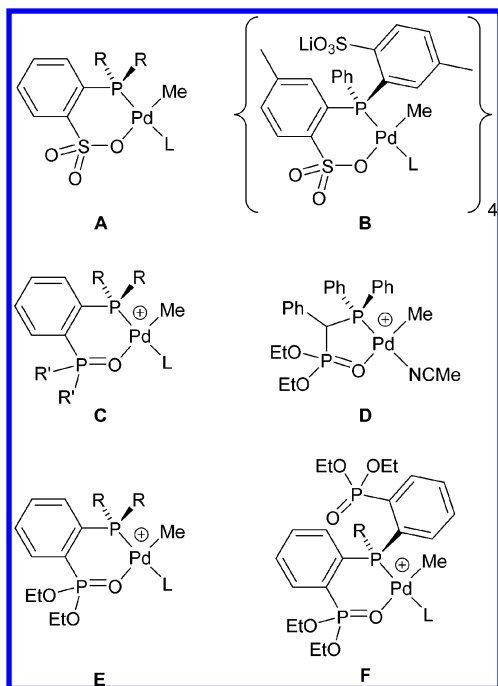
The behavior of (phosphine-bis(arenesulfonate))PdMeL catalysts ((OPO)PdMeL, B, Chart 1) differs dramatically from that of (PO)PdMeL species A. Phosphine-bis(arenesulfonate)PdMeL complexes self-assemble into tetrameric

aggregates through Li–sulfonate interactions involving the non-Pd-coordinated sulfonate moiety and one oxygen of the Pd-bound sulfonate. The tetrameric catalyst yields polyethylene with much higher molecular weight (*M_w* up to 1 000 000 Da) and incorporates more vinyl fluoride in copolymerizations compared to monomeric catalysts A. Sequestration of the Li⁺ with Crypt211 converts the tetrameric species into a mononuclear (κ²-*P,O*-OPO)PdMeL species with a pendant ArSO₃[−] group that oligomerizes ethylene with high activity, suggesting that the pendant arenesulfonate group strongly accelerates chain transfer.¹²

Bidentate phosphine-phosphine oxide ligands are similar to PO ligands in that they contain a combination of strong and weak donor groups.¹³ Cationic Pd and Ni complexes with chelating κ²-*P,O*-phosphine-phosphine oxide ligands have been shown to oligomerize ethylene, and the Pd complexes also catalyze ethylene/CO copolymerization.¹⁴ Recently, Nozaki and co-workers reported a versatile series of such catalysts (C) that polymerize ethylene to linear PE with low polydispersity and also copolymerize ethylene with allyl acetate, allyl chloride, *tert*-butylvinyl ether, vinyl acetate, and acrylonitrile, but not with methyl acrylate. Variation of the phosphine and phosphine oxide substituents (R, R') yields a broad range of catalyst activities and product molecular weights, some of which are comparable to those obtained with the phosphine-sulfonate

Received: April 28, 2014

Chart 1



catalysts.¹⁵ Phosphine-dialkyl phosphonate ligands also contain strong and weak donors.¹⁶ Braunstein found that cationic Pd-alkyl complexes (**D**) with a chelated phosphine-diethyl phosphonate ligand undergo CO insertion and subsequent ethylene or methyl acrylate insertion.^{17,18}

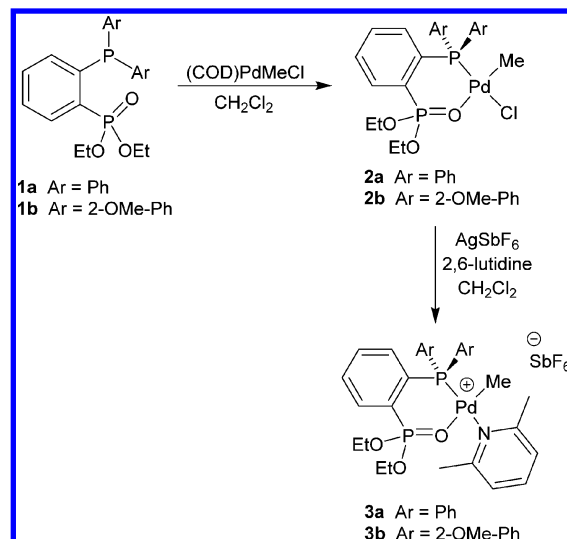
In this paper, we report the synthesis, ethylene polymerization behavior, and ethylene/acrylate copolymerization characteristics of cationic Pd complexes that contain phosphine-(diethyl phosphonate) (**E**) or phosphine-*bis*(diethyl phosphonate) (**F**) ligands. The diethyl arylphosphonate group is expected to be a weaker donor than a triaryl- or dialkylarylphosphine oxide,^{2e,19} and the presence of additional oxygen atoms may facilitate *cis/trans* isomerization of {phosphine-(diethyl phosphonate)}PdRL species, which may be important for chain growth, as proposed for the phosphine-sulfonate systems. The phosphine-*bis*(diethyl phosphonate) ligand offers the possibility of weak interactions of the non-Pd-coordinated phosphonate group with the metal or a polar comonomer, which may influence polymerization or copolymerization behavior, as observed for **B**. The second phosphonate group may also prolong catalyst lifetimes if ligand loss is a major deactivation pathway, or facilitate *cis/trans* isomerization by formation of a configurationally labile five-coordinate species.

RESULTS AND DISCUSSION

Triarylphosphine-Diethyl Phosphonate Complexes.

The benzo-linked phosphine-diethyl phosphonate ligands **1a** and **1b** (P-PO, Scheme 1) were synthesized as reported by Pringle¹⁶ⁱ and Rieger²⁰ and metalated by reaction with (COD)PdMeCl, yielding (P-PO)PdMeCl complexes **2a,2b**. The presence of P–P coupling in the ³¹P NMR spectra of the complexes is diagnostic of ligand chelation. The free ligands **1a** and **1b** do not exhibit P–P coupling, while complexes **2a** and **2b** show a *J*_{PP} of 14 and 11 Hz, respectively. Small ³J_{PH} (**2a,2b**: 4 Hz) and ²J_{PC} (**2b**: 2 Hz) values are observed for the ¹H and ¹³C PdMe resonances of **2a,2b**, consistent with a *cis* arrangement of the phosphine and methyl ligands.^{5a} The

Scheme 1



reaction of **2a,2b** with AgSbF₆ in the presence of 2,6-lutidine yields cationic (P-PO)PdMe(2,6-lut)⁺ species **3a,3b**.

The solid-state structures of **3a** and **3b** are shown in Figures 1 and 2, respectively. In each case, a square-planar Pd (II)

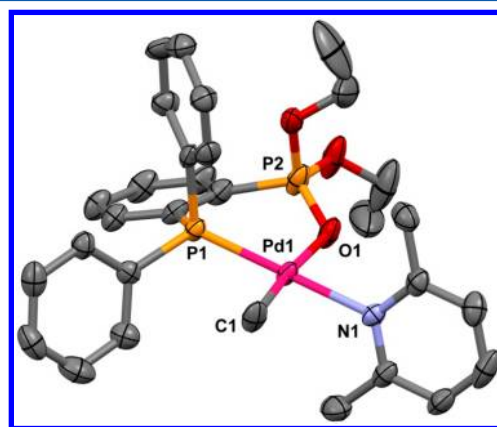


Figure 1. Molecular structure of **3a**. Hydrogen atoms and the SbF₆[−] anion are omitted. Bond lengths (Å) and angles (deg): C(1)–Pd(1) 2.020(6), N(1)–Pd(1) 2.110(4), O(1)–Pd(1) 2.170(4), P(1)–Pd(1) 2.2152(16); C(1)–Pd(1)–P(1) 88.36(17), P(1)–Pd(1)–O(1) 96.34(11), O(1)–Pd(1)–N(1) 88.29(16), N(1)–Pd(1)–C(1) 87.1(2).

center is chelated by phosphorus and oxygen donor atoms, forming a puckered six-membered ring that adopts a boat conformation in **3a** and a twist-boat conformation in **3b**. The angle between the P–C–C–P and O–Pd–P planes is 35.8° in **3a** and 33.2° in **3b**. In both complexes, the plane of the 2,6-lutidine ligand is perpendicular to the Pd square plane. The Pd–C distances of **3a** (2.020(6) Å) and **3b** (2.021(2) Å) are ca. 0.09 Å shorter than those in analogous neutral phosphine-sulfonate complexes,^{5a} presumably reflecting the weaker *trans* influence of the neutral diethyl phosphonate donor group compared to the anionic sulfonate group. The P=O distance of **3a** (1.477(4) Å) is essentially unchanged from the value reported for ligand **1a** (1.468(3) Å).¹⁶ⁱ The solution NMR data for **3a** and **3b** are consistent with the solid-state structures. Both **3a** and **3b** exhibit *J*_{PP} values of 16 Hz and ³J_{P-CH₃} values of 4 Hz, indicating κ²-P,O coordination of the P-PO ligand and a

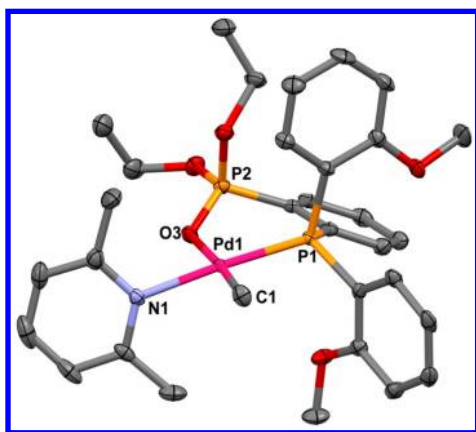
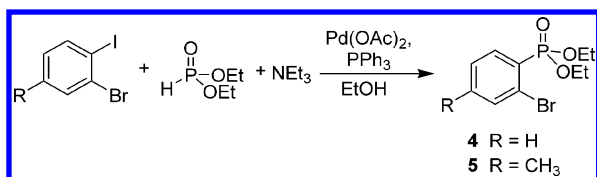


Figure 2. Molecular structure of **3b**. Hydrogen atoms and the SbF_6^- anion are omitted. Bond lengths (Å) and angles (deg): C(1)–Pd(1) 2.021(2), N(1)–Pd(1) 2.127(2), O(3)–Pd(1) 2.1639(17), P(1)–Pd(1) 2.2353(6); C(1)–Pd(1)–N(1) 92.09(9), N(1)–Pd(1)–O(3) 83.08(7), O(3)–Pd(1)–P(1) 97.45(5), P(1)–Pd(1)–C(1) 87.46(8).

cis relationship of the phosphine and methyl groups. The NMR data for **2a,2b** and **3a,3b** are consistent with fast inversion of the chelate rings on the NMR time scale for these species, which is also observed in (PO)Pd(R)(L) compounds.^{2a,21}

Diisopropylphosphine-Diethyl Phosphonate Complexes. An analogue of **1a,1b** with isopropyl substituents on the phosphine was synthesized by a different route. Diethyl *ortho*-bromo-arylphosphonates **4** and **5** were prepared by Pd-catalyzed P–C coupling²² of the appropriate aryl bromide with diethyl phosphite by Charette's procedure (Scheme 2).²³

Scheme 2



Diethyl phosphite and triethylamine were used in excess due to competing dealkylation of the former by the amine.²⁴ **5** was lithiated by metal–halogen exchange and then reacted with $\text{P}^i\text{Pr}_2\text{Cl}$, yielding ligand **1c** as a waxy solid (Scheme 3).

The reaction of **1c** with (COD)PdMeCl affords the neutral complex **2c**. Subsequent chloride abstraction by AgSbF_6 in the presence of 2,6-lutidine yielded cationic complex **3c**. Complexes **2c** and **3c** exhibit P–P coupling in the ^{31}P NMR spectra (ca. 14 Hz), whereas no P–P coupling is observed in the free ligand **1c**.

The solid-state structures of **2c** (see the Supporting Information) and **3c** (Figure 3) share several characteristics with the structures of **3a,3b**. The phosphine and diethyl phosphonate moieties chelate a square-planar Pd center. The methyl group is *cis* to the phosphine, and the 2,6-lutidine is perpendicular to the Pd square plane. The chelate ring in **3c** is notably less puckered than those in **3a** and **3b** and adopts a half-chair conformation in which the angle between P–C–C–P and O–Pd–P planes is only 13.8°. The Pd–O distance in **3c** (2.118(2) Å) is significantly shorter than those in **3a** (2.170(4) Å) and **3b** (2.1639(17) Å).

Phosphine-Bis(diethyl phosphonate) Complexes. Phosphine-bis(diethyl phosphonate) ligands **1d–1g** were

Scheme 3

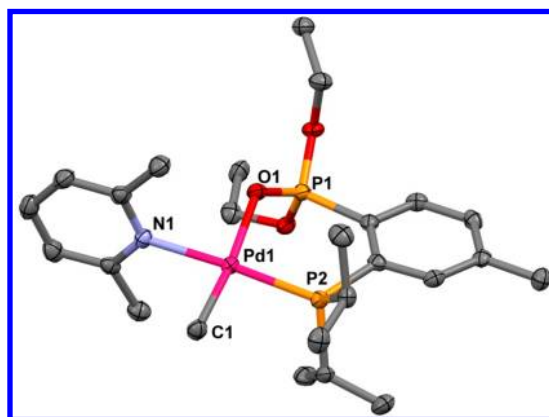
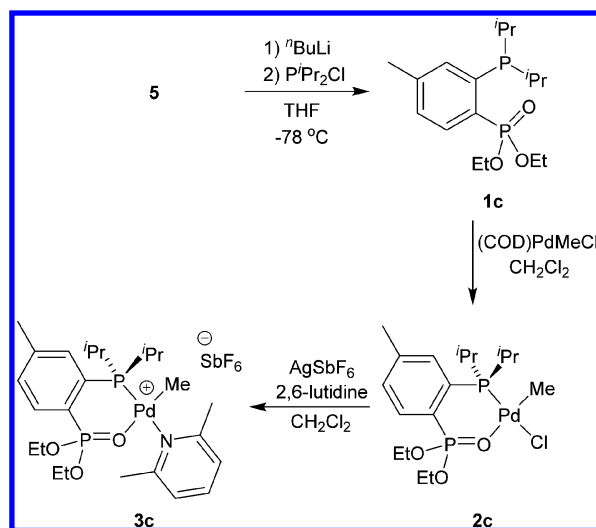
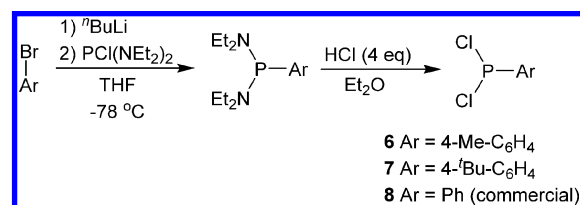


Figure 3. Molecular structure of **3c**. Hydrogen atoms and the SbF_6^- anion are omitted. Bond lengths (Å) and angles (deg): C(1)–Pd(1) 2.011(4), N(1)–Pd(1) 2.111(3), O(1)–Pd(1) 2.118(2), P(2)–Pd(1) 2.2208(14); C(1)–Pd(1)–N(1) 87.04(13), N(1)–Pd(1)–O(1) 87.44(11), O(1)–Pd(1)–P(2) 95.10(8), P(2)–Pd(1)–C(1) 90.57(11).

synthesized as shown in Schemes 4 and 5. The requisite ArPCl_2 components **6** and **7** were synthesized by lithiation of

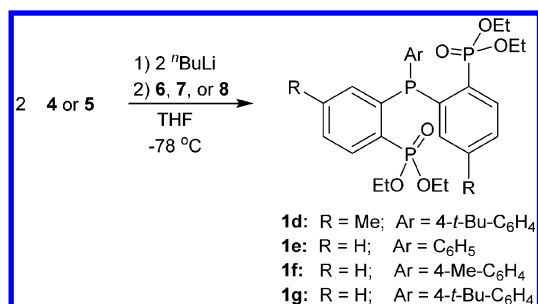
Scheme 4



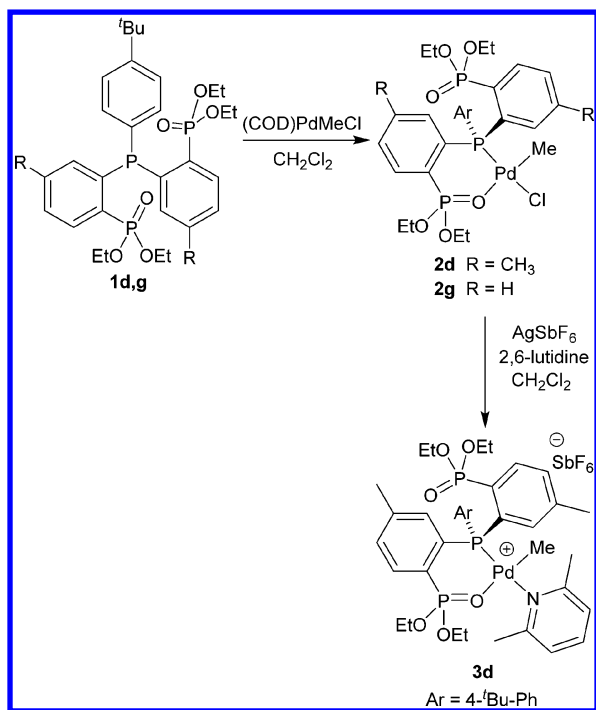
the appropriate aryl bromide, reaction with $\text{P}(\text{NEt}_2)_2\text{Cl}$, and treatment with acid (Scheme 4). Dichlorophenylphosphine (**8**) was obtained commercially. **6–8** were then coupled with 2 equiv of lithiated **4** or **5** (Scheme 5), yielding a series of phosphine-bis(diethyl phosphonate) ligands. Only **1d** and **1g**, which were expected to best solubilize subsequent Pd complexes, were used further.

The reaction of **1d,1g** with (COD)PdMeCl yields neutral (P–(PO)₂)PdMeCl complexes **2d** and **2g** (Scheme 6). In the solid

Scheme 5



Scheme 6



state, **2g** adopts a square-planar structure with coordination of the phosphine and one of the diethyl phosphonate moieties and a *cis* arrangement of the phosphine and methyl ligands (Figure 4). The noncoordinated phosphonate oxygen atom is positioned close to one axial site of the Pd center, but the P–O distance of 3.285 Å is beyond the sum of the van der Waals radii of Pd and O (3.15 Å).²⁵ The P=O bond length of the coordinated phosphonate unit (1.467(3) Å) is essentially equal to that of the noncoordinated unit (1.455(3) Å). The ¹H NMR spectra of **2d** and **2g** in CD₂Cl₂ at room temperature each contain a single set of resonances for the –Ar–P(O)(OEt)₂ rings (some are broad). The ³¹P{¹H} NMR spectra for **2d,2g** at room temperature each contain a triplet for the phosphine unit (*J*_{PP} = 9) and a single broad resonance for the phosphonate unit. These results are consistent with fast exchange on the NMR time scale of the Pd-bound and nonbound phosphonate units under these conditions.

Complex **2d** was converted to the cationic 2,6-lutidine complex **3d** by reaction with AgSbF₆ and 2,6-lutidine (Scheme 6). Repeated efforts to crystallize this material were unsuccessful. However, NMR data establish that **3d**, like **2d,2g**, contains one Pd-bound and one non-Pd-bound phosphonate group, which exchange on the NMR time scale at room temperature. At 208 K, the ¹H NMR spectrum of **3d**

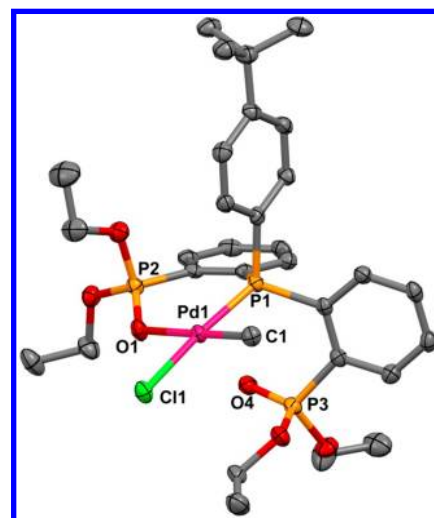


Figure 4. Molecular structure of **2g**. Hydrogen atoms are not shown. Bond lengths (Å) and angles (deg): C(1)–Pd(1) 2.011(4), Cl(1)–Pd(1) 2.3486(11), O(1)–Pd(1) 2.152(2), P(1)–Pd(1) 2.1873(11), P(2)–O(1) 1.467(3), P(3)–O(4) 1.455(3), O(4)–Pd(1) 3.285(3); C(1)–Pd(1)–Cl(1) 89.47(11), Cl(1)–Pd(1)–O(1) 88.51(7), O(1)–Pd(1)–P(1) 95.45(7), P(1)–Pd(1)–C(1) 86.70(11).

contains two sets of 2-P(O)(OEt)₂-4-Me-Ph resonances, two 2,6-lutidine methyl resonances, and two lutidine H3 resonances (Figure 5). As the temperature is raised, these corresponding sets of resonances broaden and coalesce. Similarly, the ³¹P{¹H} spectrum of **3d** at 208 K contains two doublets (*J* = 20 Hz) at δ 31.8 and 20.5, which are assigned to the phosphine and the Pd-coordinated phosphonate, and a singlet at δ 16.8, which is assigned to uncoordinated phosphonate. As the temperature is increased, the phosphine resonance evolves into a triplet with *J* = 9 Hz, and the phosphonate resonances broaden significantly. The activation barriers determined by line shape analysis of the 2-P(O)(OEt)₂-4-CH₃-Ph ¹H resonance, the lutidine-CH₃ ¹H resonance, and the ³¹P resonances are identical (Δ*G*[‡] = 14 kcal mol^{−1} at 272 K), indicative of the operation of a single dynamic process. Exchange of free and Pd-coordinated phosphonate groups will produce all of these dynamic NMR effects. Note that the 2,6-lutidine is expected to be oriented perpendicular to the Pd square plane, as observed for **3c** and **3a,3b**, and that the phosphonate exchange is sufficient to permute the lutidine methyl groups and the H3 hydrogen atoms.

Ethylene Homopolymerization by Phosphine-Diethyl Phosphonate and Phosphine-Bis(diethyl phosphonate) Complexes. Complexes **3a,3b** oligomerize/polymerize ethylene to linear low-molecular-weight PE (Table 1). At 80 °C and 28 atm ethylene, **3a** yields a Schulz–Flory distribution of C₆–C₂₂ α-olefins (>95% terminal olefins), with an activity of 125 kg mol^{−1} h^{−1} (entry 1).²⁶ The methoxy substituents in catalyst **3b** significantly alter the polymerization characteristics. Under the same conditions, for **3b**, *M*_n is increased more than 7-fold to 1760 Da, the activity is increased to 1470 kg mol^{−1} h^{−1}, and the selectivity for α-olefin (rather than internal olefin) formation upon chain transfer is 92% (entry 3). The *T*_m values for the PEs produced by **3a** (72 °C) and **3b** (126 °C) are consistent with the low molecular weights.²⁷ In comparison, the [(phosphine-phosphine oxide)PdMe(lut)][SbF₆][−] catalysts (**B**, Chart 1) reported by Nozaki exhibit activities ranging from 36 to 340 kg mol^{−1} h^{−1} when run under similar conditions (80 °C, 30 atm, in toluene), with polymer *M*_n values between 800 Da and 39

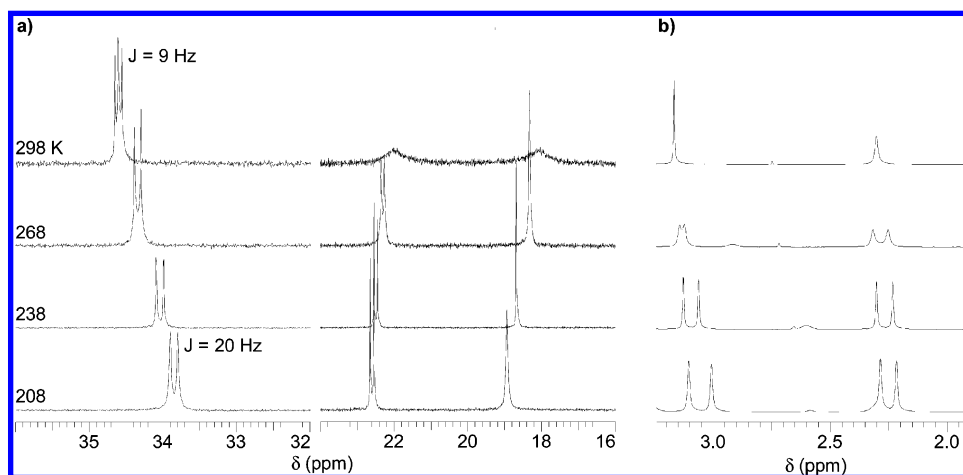


Figure 5. Variable-temperature NMR spectra of **3d**. (a) The phosphine (left) and phosphonate (right) regions of the $^{31}\text{P}\{^1\text{H}\}$ spectra. (b) The lutidine- CH_3 (downfield) and 2-P(O)(OEt) $_2$ -4- CH_3 -Ph (upfield) regions of the ^1H NMR spectra.

Table 1. Ethylene Homopolymerizations^j

entry	catalyst	pressure (atm)	$\mu\text{mol Pd}$	activity ($\text{kg mol}^{-1} \text{h}^{-1}$)	T_m ($^\circ\text{C}$)	M_n (Da) ^c	PDI ^c	% α -olefin ^f
1 ^a	3a	28	10.3	125 ^g	72.1	240 ^g	^h	97
2 ^b	3b	17	1.00	1150	125.9	1890	1.93	84
3 ^b	3b	28	1.01	1470	125.5	1760	1.99	92
4	3c	17	11.7	2.2	81.6	<570 ^h	^h	n.d. ⁱ
5	3c	28	12.9	1.0	83.9	<570	^h	n.d.
6 ^c	3c	28	13.7	<1	n.d.	n.d.	n.d.	n.d.
7 ^d	3d	17	0.85	1030	123.6	1460	1.86	10
8 ^d	3d	28	0.88	2640	123.8	1430	1.94	11

^jConditions: 80 $^\circ\text{C}$, 50 mL of toluene, 2 h. ^aAverage of four identical runs. ^bAverage of two identical runs. ^c40 $^\circ\text{C}$. ^dAverage of three identical runs. ^eDetermined by GPC, unless otherwise noted. ^f% of olefins that are α -olefins, determined by ^1H NMR. ^gDetermined by ^1H NMR analysis of soluble and insoluble polymer fractions. ^h M_n below limit for GPC analysis. ⁱNot determined.

Table 2. Ethylene/Acrylate Copolymerizations^{a,b}

entry	cat.	comon. ^d	$\mu\text{mol Pd}$	activity ($\text{kg mol}^{-1} \text{h}^{-1}$)	T_m ($^\circ\text{C}$)	M_n (Da)	PDI	comon. incorp. (mol %)	comon. % in chain	% α -olefin
1	3b	methyl acrylate (1.50 M) ^c	15.2	58	118.0	1500	2.36	1.5	95	68
2	3d	methyl acrylate (1.50 M) ^c	15.0	150	112.0	770	1.78	2.6	60	4
3	3b	acrylic acid (0.75 M)	15.1	1.2	123.7	915	3.40	0.45	32	87
4	3d	acrylic acid (0.75 M)	15.5	7.1	125.9	1465	2.46	1.1	43	70

^aConditions: 80 $^\circ\text{C}$, 28 atm ethylene, toluene, 50 mL total solution volume. ^bEach entry is the average of two identical trials. ^cWith 100 mg BHT. ^dComon. = comonomer.

kDa.¹⁵ The phosphine-diethyl phosphonates reported here, therefore, span a much broader, generally higher range of activities, but the polymer molecular weights are lower.

Surprisingly, diisopropylphosphine-diethyl phosphonate complex **3c** exhibited the lowest activity of those tested, less than 2.2 $\text{kg mol}^{-1} \text{h}^{-1}$ (entries 4–6). The small amount of polymer produced was found to have a low molecular weight ($M_n < \text{ca. } 570 \text{ Da}$).²⁸ In an effort to avoid possible catalyst decomposition at elevated temperature, a polymerization was attempted at 40 $^\circ\text{C}$, but no polymer was formed (entry 6). These results contrast with trends observed in other catalysts. The most active phosphine-phosphine oxide based catalysts within the series studied by Nozaki and co-workers were those with diisopropyl-substituted phosphines. Similarly, in phosphine-sulfonate systems, Claverie et al. found that catalysts with alkyl substituents on the phosphine are typically more active than those with aryl groups.^{2d}

The phosphine-bis(diethyl phosphonate) complex **3d** was found to be highly active for ethylene polymerization. The activity exhibits more variation with pressure than observed for **3b**, increasing from 1150 $\text{kg mol}^{-1} \text{h}^{-1}$ at 17 atm to 2640 $\text{kg mol}^{-1} \text{h}^{-1}$ at 28 atm (entries 7 and 8). The PE molecular weight varies minimally over this pressure range, from 1400 to 1500 Da, with PDI values just under 2. In contrast to phosphine-mono(diethyl phosphonate) catalysts **3a–3c**, **3d** yields a polymer with 87% internal olefins. ^{13}C NMR analysis shows that 2-olefins are the most common unsaturation (53%, *E:Z* approximately 1:1); 1-olefins (13%) and 3+-olefins (34%) were also identified. When an ethylene polymerization by **3d** was conducted in the presence of 1-heptene, the heptene was not isomerized, which implies that the internal olefins are formed during chain growth rather than by isomerization of α -olefins released by chain transfer. ^{13}C NMR analysis also revealed that the PE produced by **3d** is highly linear (less than 1 branch per 1000 C), with only methyl branches detected. The

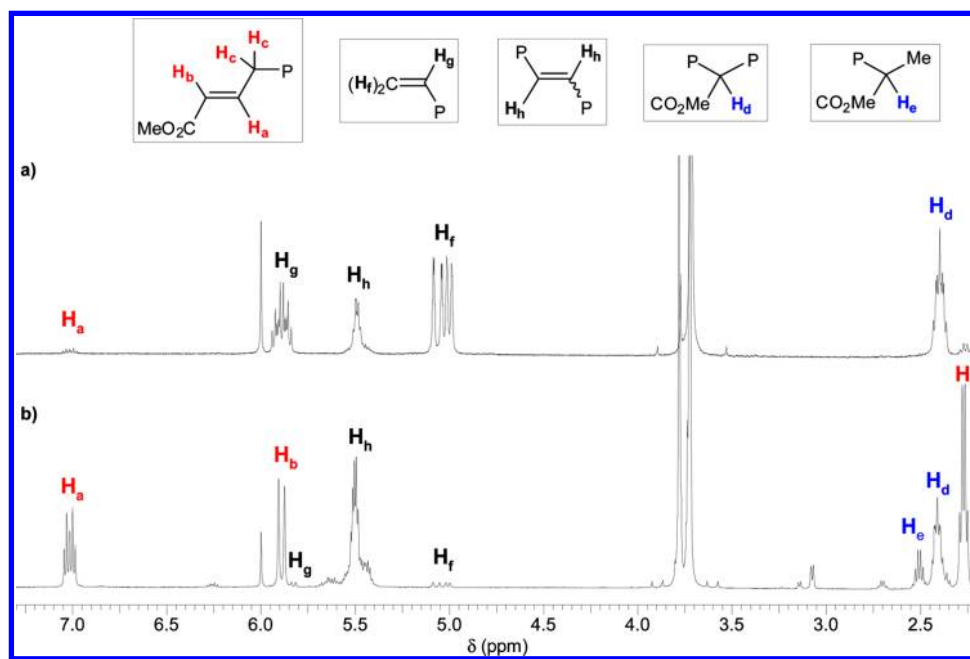


Figure 6. ^1H NMR spectra ($\text{CDCl}_2\text{CDCl}_2$, $100\text{ }^\circ\text{C}$) of ethylene/methyl acrylate copolymer produced by catalysts **3b** (a) and **3d** (b). See the Supporting Information for additional assignments.

T_m value is consistent with linear PE of the observed molecular weight.²⁷

The difference in the structures of the PEs produced by **3a,3b** (>92% α -olefin) and **3d** (>87% internal olefins) provides insight into differences in the reactivities of the growing metal alkyl species in these catalysts. For **3a,3b**, chain growth and chain transfer are fast, and either chain walking is not competitive with growth or the catalyst does not insert ethylene or undergo chain transfer from an internal alkyl position so that linear α -olefins are formed. **3d** also exhibits fast chain growth and fast chain transfer, but the predominance of internal unsaturation and the absence of branching indicate that chain walking does occur, and the resulting secondary alkyl species undergo chain transfer preferentially to chain growth.

Ethylene/Methyl Acrylate Copolymerizations. Catalysts **3b** and **3d** both incorporate methyl acrylate in ethylene copolymerizations, but with marked differences in the copolymer structure (Table 2). With both catalysts, at 28 atm ethylene, 1.50 M methyl acrylate, and $80\text{ }^\circ\text{C}$, the polymerization activity and product molecular weight are decreased relative to results for ethylene homopolymerization. Under these conditions, **3b** incorporates 1.5 mol % methyl acrylate,²⁹ and notably, the methyl acrylate is selectively (95%) incorporated in-chain, with only 5% terminating chain-end placements observed (Figure 6a). Only 5% of terminating end groups contain MA, suggesting that, after acrylate insertion, chain growth is highly favored over chain transfer. **3d** exhibits higher activity and acrylate incorporation (2.6 mol %)³⁰ but is much less selective than **3b** for in-chain acrylate placement, with only 60% incorporated in-chain and 40% incorporated into terminating chain-end groups (Figure 6b). This result indicates that, after acrylate insertion, **3d** can undergo either chain growth or chain transfer with approximately equal probability.

The ability of these phosphine-diethyl phosphonate- and phosphine-bis(diethyl phosphonate)-based catalysts to incorporate methyl acrylate is a major difference from analogous

phosphine-phosphine oxide complexes, which yielded no polymer in attempted ethylene/methyl acrylate copolymerizations.¹⁵

Ethylene/Acrylic Acid Copolymerizations. Both **3b** and **3d** copolymerize ethylene with acrylic acid (Table 2, entries 3 and 4). However, at $80\text{ }^\circ\text{C}$, 28 atm ethylene, and 0.75 M acrylic acid, the activity of both catalysts is severely depressed relative to ethylene homopolymerization. The small amount of polymer obtained with **3b** is highly contaminated with Pd black and contains 0.45 mol % acrylic acid. The molecular weight (900 Da) is substantially lower than that obtained in ethylene homopolymerization. **3d** yields copolymer containing approximately 1 mol % acrylic acid, with ca. 55% incorporated at chain ends (entry 4). Interestingly, the molecular weight of the ethylene/acrylic acid copolymer (1450 Da) is close to the value observed for ethylene homopolymerization.

CONCLUSIONS

Cationic phosphine-diethyl phosphonate complexes of the type (P-PO)PdMe(lutidine)⁺ polymerize ethylene to low-molecular-weight linear PE and copolymerize ethylene with methyl acrylate and acrylic acid. The polymerization activities of these catalysts vary widely with the substituents on the ancillary ligand. In ethylene/methyl acrylate copolymerizations, catalyst **3b** is highly selective for in-chain acrylate incorporation. Catalyst **3d** has a higher copolymerization activity and higher acrylate incorporation, but only 60% of the functionality is incorporated in-chain, with the remaining 40% as chain-end groups.

EXPERIMENTAL SECTION

General Procedures. All experiments were performed under a nitrogen atmosphere using drybox or Schlenk techniques. Nitrogen was purified by passage through columns containing Q-5 oxygen scavenger and activated molecular sieves. Methylene chloride, diethyl ether, and THF were dried by passage through columns containing activated alumina. Pentane was purified by passage through columns of BASF R3-11 oxygen scavenger and activated alumina. Compounds **1a**,

136.2 (d, $J_{PC} = 8$, C_A), 127.7 (d, $J_{PC} = 14$, C_B), 126.1 (d, $J_{PC} = 194$, C_F), 125.0 (d, $J_{PC} = 4$, C_E), 62.3 (d, $J_{PC} = 5$, -OCH₂CH₃), 21.1 (d, $J_{PC} = 1$, C_G), 16.2 (d, $J_{PC} = 7$, -OCHH₂CH₃). ESI-MS (1:1 MeOH:CH₂Cl₂, positive ion scan): 307.0 ([M + H]⁺ = 307.1), 615.1 ([2M + H]⁺ = 615.2). HRMS (*m/z*): Calcd for [C₁₁H₁₆PO₃Br + H]⁺: 307.0099, Found: 307.0099.

1-Diethylphosphonato-2-diisopropylphosphinobenzene (1c). A 100 mL Schlenk flask was charged with **5** (1.00 g, 3.25 mmol) and THF (20 mL) and cooled to -78 °C. ⁿBuLi solution (1.6 M, 2.05 mL, 3.28 mmol) was added via syringe, yielding an orange solution that was stirred for 1 h. A solution of chlorodiisopropylphosphine (0.530 g, 3.47 mmol) in THF (5 mL) was added via syringe, causing the orange color to fade. The flask was kept cold for at least 5 h and was then allowed to warm slowly overnight. The solvent was removed under reduced pressure, yielding a thick mixture of **1c** and LiCl. 25 mL of CH₂Cl₂ was added, and the resulting white suspension was filtered through Celite, yielding a clear solution. The solvent was removed under reduced pressure, yielding **1c** as an oxidatively sensitive, waxy white solid (1.02 g, 91%) after several hours. ³¹P{¹H}NMR (CD₂Cl₂): δ 19.1 (s, P=O), 3.2 (s, P). ¹H NMR (CD₂Cl₂): δ 7.86 (ddd, $J_{PH} = 13$, $J_{HH} = 8$, $J_{PH} = 3$, H_a), 7.46 (dd, $J_{PH} = 2.3$, 2.2, H_d), 7.22 (ddd, $J_{HH} = 8$, $J_{PH} = 2$, 1, H_b), 4.12 (m, -OCHH₂CH₃), 2.09 (sept. of d, $J_{HH} = 7$, $J_{PH} = 4$, P-CH(CH₃)₂), 1.32 (t, $J_{HH} = 7$, -OCHH₂CH₃), 1.15 (dd, $J_{PH} = 14$, $J_{HH} = 7$, P-CH(CH₃)₂), 0.88 (dd, $J_{PH} = 13$, $J_{HH} = 7$, P-CH(CH₃)₂). ¹³C{¹H} NMR (CD₂Cl₂): δ 143.9 (dd, $J_{PC} = 29$, 15, C_E), 142.9 (d, $J_{PC} = 3$, C_C), 135.2 (dd, $J_{PC} = 17$, 3, C_D), 135.1 (dd, $J_{PC} = 11$, 9, C_A), 134.6 (dd, $J_{PC} = 191$, 32, C_F), 130.3 (dd, $J_{PC} = 15$, 1, C_B), 63.1 (dd, $J_{PC} = 6$, 3, -OCH₂CH₃), 27.1 (d, $J_{PC} = 15$, P-CH(CH₃)₂), 22.6 (d, $J_{PC} = 2$, C_G), 21.6 (d, $J_{PC} = 13$, P-CH(CH₃)₂), 21.4 (d, $J_{PC} = 20$, P-CH(CH₃)₂), 17.6 (d, $J_{PC} = 7$, -OCHH₂CH₃). HRMS (*m/z*): Calcd for [C₁₇H₃₀P₂O₃ + H]⁺: 345.1749, Found: 345.1746.

2c. A vial was charged with **1c** (0.300 g, 0.870 mmol), (COD)PdMeCl (0.223 g, 0.841 mmol), and CH₂Cl₂ (8 mL). The resulting yellow solution was stirred for 1 h at room temperature and then filtered through Celite. Removal of the solvent under vacuum yielded a yellow solid, which was dissolved in 3 mL of CH₂Cl₂. Several small portions of this solution were used in attempted crystallizations; most of the solution was placed in a vial and layered with pentane. After several days at -40 °C, X-ray quality crystals of **2c** had formed in the vial (structure shown in the Supporting Information). These were collected on a frit, yielding **2c** as a pale yellow powder (0.152 g, 36%). This material was found to contain 0.33 equiv of CH₂Cl₂ by ¹H NMR. ³¹P{¹H}NMR (CD₂Cl₂): δ 41.6 (d, 13; P-Pd), 21.8 (d, 14; P=O). ¹H NMR (CD₂Cl₂): δ 7.74 (ddd, $J_{HH} = 8$, $J_{PH} = 8$, 3, H_a), 7.54 (t, $J_{PH} = 6$, H_d), 7.44 (d, $J_{HH} = 7$, H_b), 4.35 (m, -OCHH₂CH₃), 2.54 (sept., $J_{HH} = 7$, -CH(CH₃)₂), 2.46 (s, H_e), 1.39 (t, $J_{HH} = 7$, -OCHH₂CH₃), 1.20 (dd, $J_{HH} = 7$, $J_{PH} = 15$, -CH(CH₃)₂), 1.17 (dd, $J_{HH} = 7$, $J_{HP} = 18$, -CH(CH₃)₂), 0.74 (d, $J_{PH} = 3$, Pd-CH₃). ¹³C{¹H} NMR (CD₂Cl₂): δ 143.4 (dd, $J_{PC} = 5$, 3, C_C), 134.1 (d, $J_{PC} = 16$, C_D), 133.5 (t, $J_{PC} = 9$, C_A), 132.8 (dd, $J_{PC} = 29$, 13, C_E), 131.7 (dd, $J_{PC} = 14$, 2, C_B), 130.2 (dd, $J_{PC} = 194$, 13, C_F), 64.6 (d, $J_{PC} = 6$, -OCH₂CH₃), 25.7 (d, $J_{PC} = 26$, P-CH(CH₃)₂), 21.9 (d, $J_{PC} = 1$, C_G), 19.0 (d, $J_{PC} = 5$, P-CH(CH₃)₂), 18.5 (s, P-CH(CH₃)₂), 16.3 (d, $J_{PC} = 7$, -OCHH₂CH₃), -6.3 (d, $J_{PC} = 2$, Pd-CH₃). EA: calcd for C₁₈H₃₃P₂O₃PdCl_{0.33}CH₂Cl₂, %: C, 41.59; H, 6.40. Found: C, 41.35; H, 6.18.

3c. A vial was charged with **2c** (0.129 g, 0.256 mmol), AgSbF₆ (0.088 g, 0.255 mmol), 2,6-lutidine (30 μL, 0.258 mmol), and CH₂Cl₂ (5 mL). The resulting yellow solution was stirred for 40 min at room temperature. Filtration through Celite yielded a clear yellow solution. The solvent was removed under vacuum, yielding **3c** as a yellow solid (0.188 g, 91%, crude), which was purified by layering Et₂O onto a THF solution of **3c** and storing at -40 °C for 2 days. The resulting microcrystalline solid was collected on a frit, rinsed with Et₂O, and dried under high vacuum for 18 h. **3c** was found to contain 0.03 equiv of CH₂Cl₂ by ¹H NMR. X-ray quality crystals were grown by vapor diffusion of diethyl ether into a THF solution of **3c**. ³¹P{¹H} NMR (CD₂Cl₂): δ 41.3 (d, $J_{PP} = 14$, P-Pd), 20.1 (d, $J_{PP} = 15$, P=O). ¹H NMR (CD₂Cl₂): δ 7.78 (ddd, $J_{HH} = 8$, $J_{HP} = 8$, 4, H_a), 7.72 (t, $J_{HH} = 8$, H_d), 7.65 (t, $J_{HP} = 7$, H_c), 7.54 (dd, $J_{HH} = 8$, $J_{PH} = 1$, H_b), 7.25 (d, $J_{HH} = 8$, H_e), 4.06–3.92 (m, -OCHH₂CH₃), 3.09 (s, H_f), 2.65 (sept d, J_{HH}

= 7, $J_{HP} = 1$, P-CH(CH₃)₂), 2.52 (s, H_d), 1.35–1.25 (m, -OCHH₂CH₃ and -CH(CH₃)₂), 0.47 (d, $J_{HP} = 3$, Pd-CH₃). ¹⁹F NMR (CD₂Cl₂): δ -124.5; overlay of ¹²¹SbF₆ (sextet, $J_{SbF} = 1950$) and ¹²³SbF₆ (octet, $J_{SbF} = 1060$). ¹³C NMR (CD₂Cl₂): δ 158.8 (d, $J_{PC} = 1$, C_M), 144.7 (dd, $J_{PC} = 5$, 3, C_P), 139.3 (s, C_F), 134.9 (d, $J_{PC} = 15$, C_C), 134.5 (t, $J_{PC} = 9$, C_A), 132.5 (dd, $J_{PC} = 14$, 2, C_B), 132.2 (dd, $J_{PC} = 32$, 12, C_N), 128.4 (dd, $J_{PC} = 186$, 13, C_O), 123.4 (d, $J_{PC} = 3$, C_E), 65.2 (d, $J_{PC} = 7$, -OCH₂CH₃), 26.6 (d, $J_{PC} = 27$, P-CH(CH₃)₂), 26.4 (s, C_H), 22.0 (d, $J_{PC} = 1$, C_D), 19.3 (d, $J_{PC} = 4$, P-CH(CH₃)₂), 18.5 (s, P-CH(CH₃)₂), 16.1 (d, $J_{PC} = 7$, -OCHH₂CH₃), -6.7 (dd, $J_{PC} = 4$, 1, Pd-CH₃). ESI-MS: (CH₂Cl₂, positive ion scan): 572.0 ([M - SbF₆]⁺), 465.0 ([M - lutidine - SbF₆]⁺). EA: calcd. for C₂₃H₄₂P₂O₃NPdSbF₆·0.03 CH₂Cl₂, %: C, 37.06; H, 5.22; N, 1.73. Found: C, 37.02; H, 5.10; N, 1.78.

1d. A 500 mL Schlenk flask was charged with **5** (12.02 g, 39.14 mmol) and THF (300 mL). The flask was cooled to -78 °C, and ⁿBuLi solution (1.6 M, 26.3 mL, 42.1 mmol) was added via syringe, resulting in a deep orange-brown solution that was stirred for 20 min. A solution of **7** (4.569 g, 19.4 mmol) in THF (20 mL) was added by syringe, yielding a pale orange solution. After stirring for 40 min, the cold bath was removed, and the flask was allowed to warm to room temperature overnight, with stirring. The reaction mixture was then concentrated under reduced pressure to an orange oil, which was added to a separatory funnel with Et₂O (300 mL) and H₂O (300 mL). The aqueous layer was extracted with 3 × 100 mL of Et₂O. The combined organic layer was dried over MgSO₄, and the solvent was removed under reduced pressure to yield a viscous yellow oil. The crude product was loaded onto silica gel packed in ethyl acetate, and ethyl acetate was run through the column to remove impurities. **1d** was then eluted with a 1:11 methanol:ethyl acetate mixture. Removal of solvent under reduced pressure yielded a thick, cloudy oil. Heating at 80 °C for 7 h yielded **1d** as a white solid (5.32 g, 44%). ³¹P{¹H} NMR (CD₂Cl₂): δ 18.7 (s, P=O), -9.9 (s, P). ¹H NMR (CD₂Cl₂): δ 7.94 (ddd, $J_{PH} = 4$, $J_{HH} = 8$, $J_{PH} = 14$, H_a), 7.33 (dd, $J_{HH} = 9$, $J_{PH} = 1$, H_e), 7.23 (d, $J_{HH} = 7$, H_b), 7.03 (t, $J_{PH} = J_{HH} = 8$, H_d), 6.71 (s, H_c), 4.1–3.7 (m, -OCHH₂CH₃), 2.20 (s, H_i), 1.30 (s, H_j), 1.09 (t, $J_{HH} = 7$, -OCHH₂CH₃), 1.07 (t, $J_{HH} = 7$, -OCHH₂CH₃). ¹³C{¹H} NMR (CD₂Cl₂): δ 151.9 (s, C_Q), 142.5 (d, $J_{PC} = 3$, C_P), 142.5 (dd, $J_{PC} = 27$, 14, C_M), 136.6 (d, $J_{PC} = 16$, C_C), 135.3 (d, $J_{CP} = 12$, C_O), 135.2 (dd, $J_{PC} = 8$, 11, C_A), 134.2 (d, $J_{CP} = 21$, C_D), 131.1 (dd, $J_{PC} = 188$, 31, C_N), 129.0 (d, $J_{PC} = 15$, C_B), 125.6 (d, $J_{PC} = 7$, C_E), 62.12 (dd, $J_{PC} = 6$, 2, -OCH₂CH₃), 62.07 (dd, $J_{PC} = 6$, 2, -OCH₂CH₃), 34.9 (s, C_L), 31.4 (s, C_I), 21.7 (d, $J_{PC} = 2$, C_J), 16.29 (d, $J_{PC} = 7$, -OCHH₂CH₃), 16.26 (d, $J_{PC} = 7$, -OCHH₂CH₃). ESI-MS (1:1 MeOH:CH₂Cl₂, positive ion): 619.3 ([M + H]⁺). EA: Calcd for C₃₂H₄₅P₃O₆, %: C, 62.13; H: 7.33. Found: C, 62.10; H, 7.33.

1g. Compound **1g** was prepared analogously to **1d** from **7** and **4** and was isolated as a heavy white oil (36% yield). ¹H NMR (CD₂Cl₂): δ 8.07 (dddd, $J_{HH} = 8$, 2, $J_{PH} = 14$, 4, H_a), 7.42 (tdd, $J_{HH} = 8$, 1, $J_{PH} = 4$, H_b), 7.37 (tt, $J_{HH} = 8$, 2, $J_{PH} = 2$, H_c), 7.34 (dd, $J_{HH} = 9$, $J_{PH} = 1$, H_i), 7.05 (t, $J_{HH} = J_{PH} = 8$, H_k), 6.94 (dt, $J_{HH} = 7$, $J_{PH} = J_{PH} = 4$, H_d), 4.05–3.75 (m, -OCHH₂CH₃), 1.30 (s, -C(CH₃)₃), 1.11 (t, $J_{HH} = 7$, -OCHH₂CH₃), 1.10 (t, $J_{HH} = 7$, -OCHH₂CH₃). ³¹P{¹H} NMR (CD₂Cl₂): δ 17.4 (s, P=O), -10.6 (s, P). ¹³C{¹H} NMR (CD₂Cl₂): δ 151.9 (s, C_J), 142.6 (dd, $J_{PC} = 27$, 13, C_E), 135.9 (d, $J_{PC} = 15$, C_D), 135.2 (d, $J_{PC} = 12$, C_G), 135.1 (dd, $J_{PC} = 10$, 7, C_A), 134.4 (dd, $J_{PC} = 186$, 31, C_F), 134.2 (d, $J_{PC} = 21$, C_H), 132.1 (d, $J_{PC} = 3$, C_C), 128.3 (d, $J_{PC} = 14$, C_B), 125.7 (d, $J_{PC} = 7$, C_I), 62.2 (dd, $J_{PC} = 6$, 2, -OCH₂CH₃), 62.2 (dd, $J_{PC} = 6$, 2, -OCH₂CH₃), 34.9 (s, -C(CH₃)₃), 31.4 (s, -C(CH₃)₃), 16.3 (d, $J_{PC} = 7$, -OCHH₂CH₃), 16.2 (d, $J_{PC} = 7$, -OCHH₂CH₃). ESI-MS (1:1 MeOH:CH₂Cl₂, positive ion scan), *m/z*: 591.1 ([M + H]⁺), 607.2 ([M=O + H]⁺).

2d. A 50 mL round-bottom flask with a magnetic stir bar was charged with **1d** (1.83 g, 2.95 mmol), (COD)PdMeCl (0.770 g, 2.90 mmol), and CH₂Cl₂ (20 mL). The resulting yellow solution was stirred for 45 min, and the solvent was removed under reduced pressure, yielding a yellow solid. The solid was suspended in a mixture of Et₂O (7 mL) and pentane (13 mL), collected as a white solid, and rinsed with pentane (2 × 15 mL). Residual solvent was removed under high vacuum, yielding **2d** as a white solid (1.956 g, 87%). ³¹P{¹H}

NMR (CD_2Cl_2): δ 33.1 (t, $J_{\text{PP}} = 9$, P-Pd), 18.4 (br s, $\text{P}=\text{O}$). ^1H NMR (CD_2Cl_2): δ 7.78 (ddd, $J_{\text{PH}} = 13$, $J_{\text{HH}} = 8$, $J_{\text{PH}} = 4$, H_a), 8–7.6 (br, H_b), 7.47 (d, $J_{\text{HH}} = 8$, H_1), 7.37 (d, $J_{\text{HH}} = 8$, H_b), 6.87 (d, $J_{\text{PH}} = 5$, H_d), 4.5–3.6 (br, $-\text{OCH}_2\text{CH}_3$), 2.26 (s, H_k), 1.32 (s, $-\text{C}(\text{CH}_3)_3$), 1.25 (t, $J_{\text{HH}} = 7$, $-\text{OCH}_2\text{CH}_3$), 1.04 (br s, $-\text{OCH}_2\text{CH}_3$), 0.43 (d, $J_{\text{PH}} = 4$, Pd- CH_3). $^{13}\text{C}\{^1\text{H}\}$ NMR (CD_2Cl_2): δ 155.0 (d, $J_{\text{PC}} = 2$, C_1), 142.7 (d, $J_{\text{PC}} = 4$, C_C), 138–136 (br, C_H and C_E), 135.3 (d, $J_{\text{PC}} = 14$, C_D), 134.8 (br, C_A), 130.8 (d, $J_{\text{PC}} = 14$, C_B), 128.3 (d, $J_{\text{PC}} = 160$, C_F), 127.9 (d, $J_{\text{PC}} = 46$, C_G), 126.1 (d, $J_{\text{PC}} = 11$, C_I), 63.3 (br, $-\text{OCH}_2\text{CH}_3$), 63.0 (d, $J_{\text{PC}} = 6$, $-\text{OCH}_2\text{CH}_3$), 35.1 (d, $J_{\text{PC}} = 1$, $-\text{C}(\text{CH}_3)_3$), 31.1 (s, $-\text{C}(\text{CH}_3)_3$), 21.7 (d, $J_{\text{PC}} = 2$, C_K), 16.3 (d, $J_{\text{PC}} = 6$, $-\text{OCH}_2\text{CH}_3$), 16.0 (br d, $J_{\text{PC}} = 7$, $-\text{OCH}_2\text{CH}_3$), -3.4 (s, Pd- CH_3). ESI-MS (1:1 CH_2Cl_2 : MeOH, positive ion), m/z : 739.2 ($[\text{M} - \text{Cl}]^+$), 771.2 ($[\text{M} - \text{Cl} + \text{MeOH}]^+$). EA: Calculated for $\text{C}_{33}\text{H}_{48}\text{P}_3\text{O}_6\text{PdCl}$, %: C, 51.11; H, 6.24. Found: C, 50.89; H, 6.33.

2g. A 30 mL Schlenk tube with a magnetic stir bar was charged with **1g** (1.007 g, 1.69 mmol), (COD)PdMeCl (0.446 g, 1.68 mmol), and CH_2Cl_2 (10 mL). The resulting yellow solution was stirred for 25 min, and the solvent was removed under reduced pressure, yielding a yellow solid. The solid was suspended in Et_2O (10 mL) and collected as a white solid, which was then rinsed with Et_2O (10 mL) and then pentane (10 mL). Residual solvent was removed under high vacuum, yielding **2g** as a white solid (0.830 g, 66%). X-ray quality crystals were grown by slow evaporation of a CH_2Cl_2 solution of **2g**. $^{31}\text{P}\{^1\text{H}\}$ NMR (CD_2Cl_2): δ 32.9 (t, $J_{\text{PP}} = 9$, Pd-P), 17.5 (br, $\text{P}=\text{O}$). ^1H NMR (CD_2Cl_2): δ 7.91 (ddd, $J = 13$, 8, 4), 7.73 (br), 7.56 (m), 7.48 (td, $J = 7.5$, 1), 7.10 (br m), 4.4–3.6 (br, $-\text{OCH}_2\text{CH}_3$), 1.32 (s, $-\text{C}(\text{CH}_3)_3$), 1.26 (t, $J = 7$, $-\text{OCH}_2\text{CH}_3$), 1.04 (br s, $-\text{OCH}_2\text{CH}_3$), 0.45 (d, $J = 4$, Pd- CH_3). HRMS (m/z): Calcd for $[\text{C}_{30}\text{H}_{41}\text{P}_3\text{O}_6 + \text{H}]^+$: 591.2195, Found: 591.2192.

3d. A vial was charged with **2d** (1.003 g, 1.29 mmol), 2,6-lutidine (151 μL , 1.29 mmol), and CH_2Cl_2 (8 mL), yielding a clear solution. This solution was added to a stirred suspension of AgSbF_6 (0.444 g, 1.29 mmol) in CH_2Cl_2 (35 mL). The resulting suspension of a gray solid in a yellow supernatant was stirred for 90 min and then filtered through Celite. Solvent was removed under reduced pressure, and the resulting solid was further dried on a high-vacuum line for 19 h. Crude **3d** was isolated as a yellowish solid (1.397 g, 95%). This compound was purified by layering Et_2O onto a CH_2Cl_2 solution of **3d** and stored at -40°C for 5 days. The white precipitate was collected, rinsed with Et_2O , and dried under high vacuum for 18 h. Dynamic solution behavior of this compound at room temperature required NMR characterization at low temperature. $^{31}\text{P}\{^1\text{H}\}$ NMR (RT, CD_2Cl_2): δ 32.5 (t, $J_{\text{PP}} = 9$, Pd-P), 19.7 (br s, $\text{P}=\text{O}$), 15.9 (br s, $\text{P}=\text{O}$). $^{31}\text{P}\{^1\text{H}\}$ NMR (-60°C , CD_2Cl_2): δ 31.8 (d, $J_{\text{PP}} = 20$, Pd-P), 20.5 (d, $J_{\text{PP}} = 20$, $\text{P}=\text{O}$ -Pd), 16.8 (s, $\text{P}=\text{O}$). ^1H NMR (RT, CD_2Cl_2): δ 7.80 (br s), 7.70 (t, $J_{\text{HH}} = 8$, lut), 7.56 (d, $J = 7.5$), 7.45 (d, $J = 7.5$), 7.24 (d, $J = 7.5$), 7.1–6.6 (br), 4.4–3.4 (br, $-\text{OCH}_2\text{CH}_3$), 3.17 (s, lut- CH_3), 2.30 (s, Ar- CH_3), 1.36 (s, $-\text{C}(\text{CH}_3)_3$), 1.3–0.4 (br, $-\text{OCH}_2\text{CH}_3$), 0.16 (d, $J_{\text{H-P}} = 4$, Pd- CH_3). ^1H NMR (-60°C , CD_2Cl_2): δ 8.51 (dd, $J_{\text{PH}} = 14$, $J_{\text{HH}} = 8$, H_1), 7.79 (ddd, $J_{\text{PH}} = 13$, 4 $J_{\text{HH}} = 8$, H_a), 7.74 (ddd, $J_{\text{PH}} = 13$, 4 $J_{\text{HH}} = 8$, H_a'), 7.68 (t, $J_{\text{HH}} = 8$, H_d), 7.68 (d, $J_{\text{HH}} = 8$, H_1), 7.43 (d, $J_{\text{HH}} = 8$, H_b), 7.37 (d, $J_{\text{HH}} = 7$, H_b'), 7.32 (d, $J_{\text{HH}} = 9$, H_k), 7.24 (d, $J_{\text{HH}} = 8$, H_e), 7.17 (d, $J_{\text{HH}} = 8$, H_f), 7.02 (dd, $J_{\text{PH}} = 11$, $J_{\text{PH}} = 6$, H_c), 6.93 (dd, $J_{\text{PH}} = 8$, $J_{\text{HH}} = 8$, H_g), 6.65 (dd, $J_{\text{PH}} = 12$, 5, H_c), 4.2–3.8 (br m, $-\text{OCH}_2\text{CH}_3$), 3.55–3.20 (br m, $-\text{OCH}_2\text{CH}_3$), 3.10 (s, H_q), 3.01 (s, H_i), 2.40–2.25 (br, $-\text{OCH}_2\text{CH}_3$), 2.28 (s, H_n), 2.22 (s, H_m), 1.25 (s, H_m), 1.30–1.18 (m, $-\text{OCH}_2\text{CH}_3$), 1.01 (t, $J_{\text{HH}} = 7$, $-\text{OCH}_2\text{CH}_3$), 0.48 (t, $J_{\text{HH}} = 7$, $-\text{OCH}_2\text{CH}_3$), -0.01 (d, $J_{\text{PH}} = 3$, Pd- CH_3). ^{13}C NMR (-60°C , CD_2Cl_2): δ 158.3 (s, $\text{C}_{\text{O/P}}$), 158.1 (s, $\text{C}_{\text{O/P}}$), 154.3 (s, C_K), 143.3 (d, $J_{\text{PC}} = 6$, C_S), 142.5 (d, $J_{\text{PC}} = 8$, C_S'), 138.4 (d, $J_{\text{PC}} = 23$, C_I), 138.3 (s, C_D), 137.0 (dd, $J_{\text{PC}} = 47$, 12, C_T), 135.8–135.4 (m, C_C), 135.0 (m, C_A), 134.0 (d, $J_{\text{PC}} = 12$, C_C'), 133.9 (br m, C_A'), 132.9 (s, C_G), 132.5 (dd, $J_{\text{PC}} = 51$, 16, C_T'), 131.1 (d, $J_{\text{PC}} = 13$, C_B), 130.2 (d, $J_{\text{PC}} = 13$, C_B'), 126.3 (dd, $J_{\text{PC}} = 188$, 12, C_U), 125.9 (d, $J_{\text{PC}} = 16$, C_I), 125.8 (s, C_H), 125.1 (d, $J_{\text{PC}} = 49$, C_V), 123.1 (dd, $J_{\text{PC}} = 185$, 18, C_U'), 122.3 (s, C_E), 122.2 (s, C_F), 62.9 (d, $J_{\text{PC}} = 6$, $-\text{OCH}_2\text{CH}_3$), 62.7 (d, $J_{\text{PC}} = 6$, $-\text{OCH}_2\text{CH}_3$), 61.5 (d, $J_{\text{PC}} = 6$, $-\text{OCH}_2\text{CH}_3$), 61.3 (d, $J_{\text{PC}} = 6$, $-\text{OCH}_2\text{CH}_3$), 34.5 (s, C_L), 30.2 (s, C_M), 26.2 (s, C_Q), 25.8 (s, C_R), 21.4 (s, C_N), 21.3 (s, C_N'), 15.7 (d, J_{PC}

$= 7$, $-\text{OCH}_2\text{CH}_3$), 15.4 (d, $J_{\text{PC}} = 8$, $-\text{OCH}_2\text{CH}_3$), 14.6 (d, $J_{\text{PC}} = 9$, $-\text{OCH}_2\text{CH}_3$), -6.0 (d, $J_{\text{PC}} = 4$, Pd- CH_3). ^{19}F NMR (RT, CD_2Cl_2): δ -124.6 ; overlay of $^{121}\text{SbF}_6$ (sextet, J_{SbF} of 2050) and $^{123}\text{SbF}_6$ (octet, $J_{\text{SbF}} = 1110$). ESI-MS (1:1 CH_2Cl_2 : MeOH, positive ion, fragmentor 40), m/z : 845.3 [$\text{M} - \text{SbF}_6 - \text{H}$], 738.1 [$\text{M} - \text{SbF}_6 - \text{lut} - \text{H}$]. EA: Calcd for $\text{C}_{40}\text{H}_{57}\text{P}_3\text{O}_6\text{NPdSbF}_6$, %: C, 44.36; H, 5.31; N, 1.29. Found: C, 44.09; H, 5.15; N, 1.36.

Ethylene Homopolymerizations. In a glovebox, a 200 mL glass autoclave liner was charged with a solution of the catalyst in CH_2Cl_2 (ca. 1 mL). The solvent was removed under vacuum, and toluene (50 mL) was added. For catalyst loadings larger than 5 μmol , the catalyst was weighed directly into the liner. The glass liner was placed in a stainless steel autoclave, which was sealed and removed from the glovebox. The autoclave was heated to (typically) 80°C and pressurized with ethylene while the contents were stirred. After 2 h, the autoclave was cooled to 25°C and vented. Acetone (50 mL) was added to precipitate polymer. The polymer was collected by filtration, rinsed with acetone, and dried overnight in a vacuum oven. The oligomer content of the filtrate was determined by GC–MS analysis.

Ethylene Copolymerizations with Methyl Acrylate or Acrylic Acid. In a glovebox, a 200 mL glass autoclave liner was charged with catalyst, toluene (50 mL), and, if applicable, BHT (0.100 g). Comonomer was added, and the liner was placed in a stainless steel autoclave, which was sealed and removed from the glovebox. Stirring was initiated, the autoclave was pressurized with ethylene (22 atm), and the ethylene line was closed. The autoclave was heated to 80°C , and the pressure was adjusted to 28 atm with ethylene on demand. After the listed polymerization time, the autoclave was cooled and vented. MeOH (200 mL, methyl acrylate copolymerization) or 10% $\text{H}_2\text{O}/90\%$ MeOH solution (200 mL, acrylic acid copolymerization) was added to precipitate the polymer. The solid was collected by filtration and washed with the corresponding solvent. For the acrylic acid copolymerization, the polymer was then washed with MeOH. All samples were then dried overnight in a vacuum oven.

ASSOCIATED CONTENT

Supporting Information

Crystal structure report for compounds **2g**, **3c**, **2c**, **3b**, and **3a**; synthesis of compounds; NMR labeling scheme; molecular structure of complex **2c**; ethylene homopolymerization data; Schulz–Flory analysis of oligomers from **3a**; 1-heptene isomerization experiment; ethylene copolymerization data; variable-temperature NMR spectra of **3d**; NMR spectra of compounds, oligomer fraction, and polymers; and crystallographic data in CIF format. This material is available free of charge via the Internet at <http://pubs.acs.org>.

AUTHOR INFORMATION

Notes

The authors declare no competing financial interest.

ACKNOWLEDGMENTS

This work was supported by the National Science Foundation (DGE-1144082, CHE-0911180, and CHE-1048528).

REFERENCES

- (1) (a) Nakamura, A.; Ito, S.; Nozaki, K. *Chem. Rev.* **2009**, *109*, 5215. (b) Nakamura, A.; Anselment, T. M.; Claverie, J.; Goodall, B.; Jordan, R. F.; Mecking, S.; Rieger, B.; Sen, A.; van Leeuwen, P. W.; Nozaki, K. *Acc. Chem. Res.* **2013**, *46*, 1438.
- (2) (a) Vela, J.; Lief, G. R.; Shen, Z.; Jordan, R. F. *Organometallics* **2007**, *26*, 6624. (b) Wucher, P.; Goldbach, V.; Mecking, S. *Organometallics* **2013**, *32*, 4516. (c) Anselment, T. M. J.; Wichmann, C.; Anderson, C. E.; Herdtweck, E.; Rieger, B. *Organometallics* **2011**, *30*, 6602. (d) Piche, L.; Daigle, J. C.; Rehse, G.; Claverie, J. P. *Chem.—Eur. J.* **2012**, *18*, 3277. (e) Neuwald, B.; Ölscher, F.; Göttker-Schnetmann, I.; Mecking, S. *Organometallics* **2012**, *31*, 3128.

- (3) (a) Drent, E.; van Dijk, R.; van Ginkel, R.; van Oort, B.; Pugh, R. *I. Chem. Commun.* **2002**, 744. (b) Guironnet, D.; Roesle, P.; Runzi, T.; Gottker-Schnetmann, L.; Mecking, S. *J. Am. Chem. Soc.* **2009**, *131*, 422. (c) Kochi, T.; Yoshimura, K.; Nozaki, K. *Dalton Trans.* **2006**, 25. (d) Skupov, K. M.; Marella, P. R.; Simard, M.; Yap, G. P. A.; Allen, N.; Conner, D.; Goodall, B. L.; Claverie, J. P. *Macromol. Rapid Commun.* **2007**, *28*, 2033.
- (4) (a) Wucher, P.; Roesle, P.; Falivene, L.; Cavallo, L.; Caporaso, L.; Göttker-Schnetmann, L.; Mecking, S. *Organometallics* **2012**, *31*, 8505. (b) Kryuchkov, V. A.; Daigle, J. C.; Skupov, K. M.; Claverie, J. P.; Winnik, F. M. *J. Am. Chem. Soc.* **2010**, *132*, 15573. (c) Skupov, K. M.; Hobbs, J.; Marella, P.; Conner, D.; Golisz, S.; Goodall, B. L.; Claverie, J. P. *Macromolecules* **2009**, *42*, 6953. (d) Runzi, T.; Frohlich, D.; Mecking, S. *J. Am. Chem. Soc.* **2010**, *132*, 17690. (e) Daigle, J.-C.; Piche, L.; Claverie, J. P. *Macromolecules* **2011**, *44*, 1760.
- (5) (a) Kochi, T.; Noda, S.; Yoshimura, K.; Nozaki, K. *J. Am. Chem. Soc.* **2007**, *129*, 8948. (b) Luo, S.; Vela, J.; Lief, G. R.; Jordan, R. F. *J. Am. Chem. Soc.* **2007**, *129*, 8946. (c) Ito, S.; Munakata, K.; Nakamura, A.; Nozaki, K. *J. Am. Chem. Soc.* **2009**, *131*, 14606.
- (6) (a) Weng, W.; Shen, Z.; Jordan, R. F. *J. Am. Chem. Soc.* **2007**, *129*, 15450. (b) Leicht, H.; Gottker-Schnetmann, L.; Mecking, S. *Angew. Chem., Int. Ed.* **2013**, *52*, 3963. (c) Borkar, S.; Newsham, D. K.; Sen, A. *Organometallics* **2008**, *27*, 3331.
- (7) (a) Bouilhac, C.; Rünzi, T.; Mecking, S. *Macromolecules* **2010**, *43*, 3589. (b) Skupov, K. M.; Piche, L.; Claverie, J. P. *Macromolecules* **2008**, *41*, 2309.
- (8) (a) Ravasio, A.; Boggioni, L.; Tritto, I. *Macromolecules* **2011**, *44*, 4180. (b) Ito, S.; Kanazawa, M.; Munakata, K.; Kuroda, J.; Okumura, Y.; Nozaki, K. *J. Am. Chem. Soc.* **2011**, *133*, 1232. (c) Nakamura, A.; Munakata, K.; Ito, S.; Kochi, T.; Chung, L. W.; Morokuma, K.; Nozaki, K. *J. Am. Chem. Soc.* **2011**, *133*, 6761.
- (9) (a) Britovsek, G. J. P.; Gibson, V. C.; Wass, D. F. *Angew. Chem., Int. Ed.* **1999**, *38*, 428. (b) Gibson, V. C.; Spitzmesser, S. K. *Chem. Rev.* **2003**, *103*, 283.
- (10) Noda, S.; Nakamura, A.; Kochi, T.; Chung, L. W.; Morokuma, K.; Nozaki, K. *J. Am. Chem. Soc.* **2009**, *131*, 14088.
- (11) (a) Berkefeld, A.; Mecking, S. *Angew. Chem., Int. Ed.* **2008**, *47*, 2538. (b) Luo, S.; Jordan, R. F. *J. Am. Chem. Soc.* **2006**, *128*, 12072. (c) Chen, C.; Jordan, R. F. *J. Am. Chem. Soc.* **2010**, *132*, 10254. (d) Chen, C.; Luo, S.; Jordan, R. F. *J. Am. Chem. Soc.* **2010**, *132*, 5273. (e) Kilyanek, S. M.; Stoebenau, E. J.; Vinayavekhin, N.; Jordan, R. F. *Organometallics* **2010**, *29*, 1750.
- (12) (a) Shen, Z.; Jordan, R. F. *J. Am. Chem. Soc.* **2010**, *132*, 52. (b) Shen, Z. L.; Jordan, R. F. *Macromolecules* **2010**, *43*, 8706.
- (13) (a) Coyle, R. J.; Slovokhotov, Y. L.; Antipin, M. Y.; Grushin, V. V. *Polyhedron* **1998**, *17*, 3059. (b) Al-Jibori, S. A.; Amin, O. H.; Al-Allaf, T. A. K.; Davis, R. *Transition Met. Chem.* **2001**, *26*, 186. (c) Sgarbossa, P.; Pizzo, E.; Scarso, A.; Sbovata, S. M.; Michelin, R. A.; Mozzon, M.; Strukul, G.; Benetollo, F. *J. Organomet. Chem.* **2006**, *691*, 3659.
- (14) (a) Brassat, I.; Keim, W.; Killat, S.; Möthra, M.; Mastroilli, P.; Nobile, C. F.; Suranna, G. P. *J. Mol. Catal. A: Chem.* **2000**, *157*, 41. (b) Mecking, S.; Keim, W. *Organometallics* **1996**, *15*, 2650.
- (15) (a) Carrow, B. P.; Nozaki, K. *J. Am. Chem. Soc.* **2012**, *134*, 8802. (b) Carrow, B. P.; Nozaki, K. *Macromolecules* **2014**, *47*, 2541.
- (16) (a) Bischoff, S.; Kant, M. *Catal. Today* **2001**, *66*, 183. (b) Bischoff, S.; Weigt, A.; Mießner, H.; Lücke, B. *J. Mol. Catal. A: Chem.* **1996**, *107*, 339. (c) Weigt, A.; Bischoff, S. *Phosphorus, Sulfur Silicon Relat. Elem.* **1995**, *102*, 91. (d) Bischoff, S.; Kant, M. *Ind. Eng. Chem. Res.* **2000**, *39*, 4908. (e) Schull, T. L.; Fettingner, J. C.; Knight, D. A. *J. Chem. Soc., Chem. Commun.* **1995**, 1487. (f) Schull, T. L.; Fettingner, J. C.; Knight, D. A. *Inorg. Chem.* **1996**, *35*, 6717. (g) Ganguly, S.; Mague, J. T.; Roundhill, D. M. *Inorg. Chem.* **1992**, *31*, 3500. (h) Machnitzki, P.; Nickel, T.; Stelzer, O.; Landgrafe, C. *Eur. J. Inorg. Chem.* **1998**, 1029. (i) Ellis, D. D.; Harrison, G.; Orpen, A. G.; Phetmung, H.; Pringle, P. G.; deVries, J. G.; Oevering, H. *Dalton Trans.* **2000**, 671.
- (17) (a) Morise, X.; Braunstein, P.; Welter, R. C. *R. Chim.* **2003**, *6*, 91. (b) Oberbeckmann-Winter, N.; Morise, X.; Braunstein, P.; Welter, R. *Inorg. Chem.* **2005**, *44*, 1391. (c) Hamada, A.; Braunstein, P. *Inorg. Chem.* **2009**, *48*, 1624.
- (18) Hamada, A.; Braunstein, P. *Organometallics* **2009**, *28*, 1688.
- (19) Derencsenyi, T. T. *Inorg. Chem.* **1981**, *20*, 665.
- (20) Reisinger, C. M.; Nowack, R. J.; Volkmer, D.; Rieger, B. *Dalton Trans.* **2007**, 272.
- (21) Neuwald, B.; Caporaso, L.; Cavallo, L.; Mecking, S. *J. Am. Chem. Soc.* **2013**, *135*, 1026.
- (22) (a) Hirao, T.; Masunaga, T.; Ohshiro, Y.; Agawa, T. *Synthesis* **1981**, 56. (b) Hirao, T.; Masunaga, T.; Yamada, N.; Ohshiro, Y.; Agawa, T. *Bull. Chem. Soc. Jpn.* **1982**, *55*, 909. (c) Gooßen, L. J.; Dezfūli, M. K. *Synlett* **2005**, 445.
- (23) Bonnaventure, I.; Charette, A. B. *J. Org. Chem.* **2008**, *73*, 6330.
- (24) (a) Bryant, D. E.; Kilner, C.; Kee, T. P. *Inorg. Chim. Acta* **2009**, *362*, 614. (b) Gray, M. D. M.; Smith, D. J. H. *Tetrahedron Lett.* **1980**, *21*, 859. (c) Belabassi, Y.; Alzghari, S.; Montchamp, J. L. *J. Organomet. Chem.* **2008**, *693*, 3171. (d) Georgiev, E. M.; Tsevi, R.; Vassileva, V.; Troev, K.; Roundhill, D. M. *Phosphorus, Sulfur Silicon Relat. Elem.* **1994**, *88*, 139. (e) Troev, K.; Borisov, G. *Phosphorus, Sulfur Silicon Relat. Elem.* **1987**, *29*, 129.
- (25) Bondi, A. *J. Phys. Chem.* **1964**, *68*, 441.
- (26) The M_n and activity data are for the total product (insoluble and soluble fractions). The soluble fraction was analyzed by GC/MS and found to contain a Schulz–Flory distribution of oligomers ($\alpha = 0.87$; $\beta = 0.15$).
- (27) (a) Mandelkern, L.; Prasad, A.; Alamo, R. G.; Stack, G. M. *Macromolecules* **1990**, *23*, 3696. (b) Prasad, A.; Mandelkern, L. *Macromolecules* **1989**, *22*, 914. (c) Stack, G. M.; Mandelkern, L.; Voigt-Martin, I. G. *Macromolecules* **1984**, *17*, 321.
- (28) A small amount of oligomeric material was detected by GC–MS but was not included in the calculation of the activity and M_n .
- (29) On average, each chain contains 0.78 MA units
- (30) On average, each chain contains 0.68 MA units
- (31) Rulke, R. E.; Ernsting, J. M.; Spek, A. L.; Elsevier, C. J.; van Leeuwen, P. W. N. M.; Vrieze, K. *Inorg. Chem.* **1993**, *32*, 5769.
- (32) De Graaf, W.; Boersma, J.; Smeets, W. J. J.; Spek, A. L.; Van Koten, G. *Organometallics* **1989**, *8*, 2907.
- (33) Punji, B.; Mague, J. T.; Balakrishna, M. S. *Inorg. Chem.* **2007**, *46*, 10268.
- (34) Galland, G. B.; de Souza, R. F.; Mauler, R. S.; Nunes, F. F. *Macromolecules* **1999**, *32*, 1620.